Available online at www.sciencedirect.com
ScienceDirect
Ceramics International 35 (2009) 2161–2169
CERAMICS INTERNATIONAL
www.elsevier.com/locate/ceramint

Three-dimensional carbon fiber-reinforced silicon carbide matrix composites by vapor silicon infiltration

Qing Zhou [a,b], Shaoming Dong [a,*], Yusheng Ding [a], Zhen Wang [a,b], Zhengren Huang [a], Dongliang Jiang [a]

[a] *Shanghai Institute of Ceramics, Chinese Academy of Sciences, Shanghai 200050, China*
[b] *Graduate School of the Chinese Academy of Sciences, Beijing 100049, China*

Received 27 February 2008; received in revised form 6 October 2008; accepted 26 November 2008
Available online 13 January 2009

Abstract

Three-dimensional carbon fiber-reinforced SiC matrix composites (C_f/SiC) were fabricated by vapor silicon infiltration (VSI) successfully. Scanning electron microscopy (SEM), transmission electron microscopy (TEM) and wavelength dispersive spectrometer (WDS) analysis revealed that the microstructure and composition of constituent phases are strongly dependent on temperature. At 1973 K, the obtained C_f/SiC composite mainly consists of SiC, carbon fiber and residual Si, and shows a densified microstructure. The flexural tests show non-catastrophic fracture behavior for composites fabricated by VSI process, and the ultimate flexural stress is comparable to those of composites fabricated by other processing techniques, demonstrating VSI is an effective way to fabricate the dense C_f/SiC composites with good mechanical properties.

Keywords: B. Composites; B. Fiber; D. SiC

1. Introduction

Because of their superior damage tolerance and excellent thermo-mechanical properties, carbon fiber-reinforced silicon carbide matrix composites (C_f/SiC) have received considerable attention and have been regarded as one of the most potential structural materials for high temperature technologies, such as advanced energy-generation systems and aerospace-propulsion systems [1–4].

So far, there are several processing techniques which have been developed to fabricate the short/continuous carbon fiber-reinforced SiC matrix composite, for instance, chemical vapor infiltration (CVI), polymer impregnation and pyrolysis (PIP), or reaction sintering (RS).

Each of these processes showed advantages and disadvantages in terms of properties and cost-effectiveness. In comparison to CVI/PIP techniques, RS has been demonstrated to be a cost-effective method, and has been used to fabricate SiC-based composites with good properties and complex shapes [5,6]. In general, RS process is mainly focusing on the liquid silicon infiltration (LSI) technique. By LSI technique, the residual open pores and cracks are filled with liquid silicon. Simultaneously, the infiltrated liquid silicon reacts with carbon to form the silicon carbide matrix [7,8]. Until now, the fabrication and characterization of SiC composites by LSI technique have been extensively investigated experimentally and theoretically, but the other way by vapor silicon infiltration (VSI) is rarely studied in the fabrication of matrix of the SiC composites.

Theoretically, vapor silicon is much easier to infiltrate into the open pores/cracks than liquid silicon. To a large extent, vapor silicon infiltration avoids the clogging of infiltrating channels and the generation of structural defects/flaws. Furthermore, in order to satisfying with the requirements from engineering application, the amount of SiC matrix formed by the reaction between silicon and carbon could be controlled by changing the processing parameters.

Under this consideration, in the present work, efforts were made to fabricate three-dimensional (3D) carbon fiber-reinforced SiC matrix composites by VSI process. Also, the microstructural features and phase compositions on composites fabricated at different infiltration temperatures were analyzed

* Corresponding author. Tel.: +86 21 5241 4324; fax: +86 21 5241 3903.
E-mail address: smdong@mail.sic.ac.cn (S. Dong).

0272-8842/$34.00
doi:10.1016/j.ceramint.2008.11.023

by X-ray diffractometer (XRD), scanning electron microscopy (SEM) and transmission electron microscopy (TEM). The fracture properties were evaluated by three-point bending test. The oxidation resistance was studied by isothermal exposure tests in air and thermo-gravimetric data (TG–DSC) analysis.

2. Experimental

Firstly, a bi-layered PyC–SiC coating acting as interphase was deposited on the 3D woven carbon fiber fabrics (M40JB, Toray, Tokyo, Japan) by FP-CVI [9] using methane and MTS/H_2 as precursors. The 3D preform architecture had a fiber distribution of 8:2:1 in the x:y:z directions, respectively, and a ~40% fiber overall volume fraction. Then the coated fabrics were impregnated by a slurry containing nano-SiC particles (about 60 nm in size, Kiln Nanometer Technology Development Co. Ltd., China) and a phenolic resin, followed by pyrolysis at 2073 K in case of volatile when VSI at high temperature, to make a carbon fiber-reinforced composite (CFC) containing carbon matrix. Such composites contained large number of pores and cracks.

In order to fabricate the carbon fiber-reinforced SiC matrix composite (C_f/SiC) by VSI process, a silicon powder (purity: 99.9%, grain size: 75 μm, Sinopharm Chemical Reagent Co., Ltd., Shanghai, China) was put inside a graphite crucible, then the CFC composite was put above the silicon powder (Fig. 1). Finally, the graphite crucible with silicon powder and CFC composite were sealed and heated up to the desired infiltration temperature to form the silicon carbide matrix by VSI.

The desired infiltration temperature was reached at a heating rate of 10 K/min. In this work, VSI was conducted at high temperature (1873–1973 K) for 3 h in vacuum (residual pressure ~1 Pa). During silicon infiltration process, the silicon vapor pressure was estimated based on the Antoine equation [10]:

$$\log P = -\frac{A}{T+C} + B \tag{1}$$

where P and T are the gas pressure in bar (with 1 bar ≈ 10^5 Pa) and temperature (K), A, B and C are constants. When temperature is 1997–2560 K, values of A, B and C are 9.56436, 23308.848 and −123.133, respectively. At 1973 K, the state of silicon is very similar to perfect gas. By using Eq. (1), the silicon vapor pressure was estimated to be about 100 Pa. Such silicon vapor could easily diffuse into open pores/cracks, and spontaneously react with carbon to form the SiC.

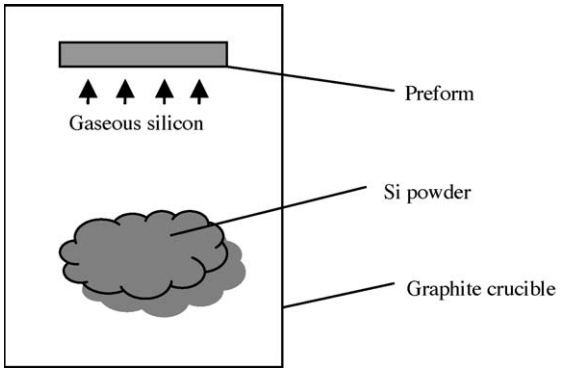

Fig. 1. Experimental set-up for vapor silicon infiltration.

The density (Vd) and porosity (Pe) of C_f/SiC composites obtained by VSI process were measured by Archimedes' method:

$$\mathrm{Vd} = \frac{M1 \times DT}{M3 - M2} \tag{2}$$

$$\mathrm{Pe}\,(\%) = \frac{M3 - M1}{M3 - M2} \times 100 \tag{3}$$

where $M1$ is the weight of composites at room temperature. Keeping the composites in boiling water for 3 h. After cooling down to room temperature, the weight ($M2$) is measured in the water at room temperature. The weight ($M3$) is measured after removing water from the surface. In Eq. (2), density (g/cm^3) of water at T is needed.

The samples were cut and ground into about 35 mm in x direction, 4 mm in y direction and 2.5 mm in z for fracture property testing. Sets of four specimens were employed for flexure strength tests of each sample, with the aim of obtain average values. The fracture properties were estimated by three-point bending test with a supporting span of 24 mm and a crosshead speed of 0.5 mm/min on an INSTRON test machine (Mode: 5566, Canton, MA, USA). The volume fraction of silicon in composite was estimated according to the mass change before and after etching in an aqueous solution of 70 wt% HF + 30 wt% HNO_3.

The constituent phases of the as-fabricated C_f/SiC composites were determined by X-ray diffractometer (XRD, Mode: RAX-10, Rigaku, Japan) with Cu Kα radiation. The microstructure and element mapping of composites were characterized by electron probe microanalyzer (EPMA, Mode: JXA-8100, JEOL, Tokyo, Japan) with wavelength dispersive spectrometer (WDS). In addition, the morphologies and chemical information of composites fabricated at different infiltration temperatures were analyzed by scanning electron microscopy and transmission electron microscopy (TEM, Mode: JEM-2100F, JEOL, Tokyo, Japan).

In order to evaluate the oxidation resistance, the weight change after isothermal exposure in air at 1273 K was measured. The isothermal exposure tests were carried out in muffle furnace and the heating rate was 10 K/min. Additionally, the TG–DSC data analysis of the composites was performed by NETZSCH simultaneous thermal analyzer (STA449C Jupiter, Germany) in air at elevated temperatures.

3. Results

3.1. Microstructure and constituent phase analysis

Figs. 2 and 3 show the crosssection of as-fabricated C_f/SiC composites by VSI process at different infiltration temperatures. It is obvious that macropores are observed in the inter-bundle area for composites fabricated at 1873 K and 1923 K as shown in Fig. 2(a) and (b). Meanwhile, the size of macropores

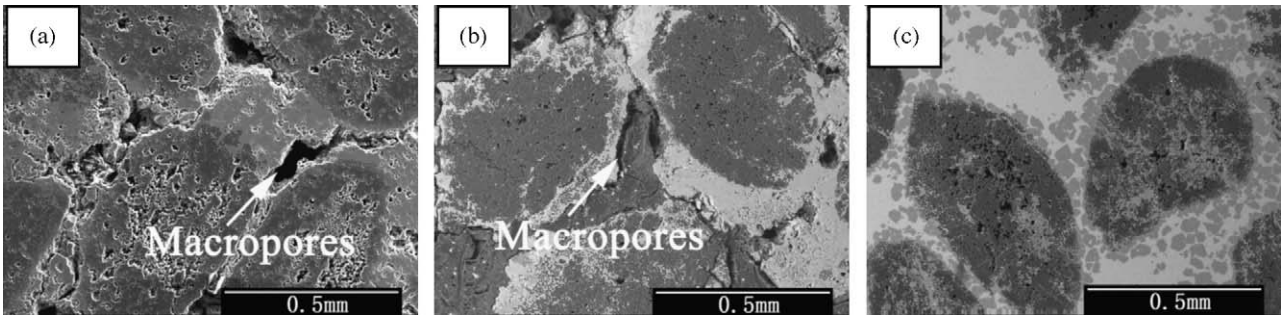

Fig. 2. Morphologies of crosssection of the C_f/SiC composites fabricated by VSI process at different infiltration temperatures: (a) 1873 K; (b) 1923 K; (c) 1973 K.

decreased with increasing the infiltration temperature. It should be noted that the macropores tend to be formed easily in the inter-bundle area, but not the intra-bundle area. However, for C_f/SiC composites fabricated at 1973 K, the inter-bundle area shows densified microstructure even though some micropores are observed as shown in Fig. 2(c), illuminating that the VSI can fill the large inter-bundle pores. Such densified microstructure is also observed in the intra-bundle area in composites fabricated at 1973 K as shown in Fig. 3. The porosity of composites made at 1973 K was evaluated to be about 6% by using Eq. (3), showing that relatively dense matrix can be achieved by VSI.

Fig. 4 shows the XRD diffraction pattern of a composite fabricated by VSI process at 1973 K. It can be seen that the composite consists of β-SiC, Si and carbon phases. The β-SiC lines show strong intensity, indicating large amount of SiC matrix is formed after VSI process. In addition, after etching the composite in the acid solution of 70 wt% HF + 30 wt% HNO_3, the residual Si was removed as shown in the lower XRD diffraction pattern of Fig. 4. This information is very useful to estimate how much silicon is reacted with carbon during the VSI process. While the residual carbon derived from resin will be investigated by WDS.

Fig. 5 shows the TEM data. It is found that both residual Si and formed SiC grains appear in large crystals which are about a few micrometers. The selected area diffraction (SAD) patterns show Si and SiC grains have perfect crystallographic orientations. SiC formed during reaction has clear (1 1 1) and (2 2 0) spots, indicating that the product is high quality β-SiC. SAD patterns of Si show its (1 1 1) and $(1\,1\,\bar{1})$ spots.

In order to investigate the homogeneity of SiC formation in composites by VSI process at different infiltration temperatures, element mappings were performed on the polished crosssection of composites by WDS.

Fig. 6(a) and (b) shows the carbon and silicon mappings of the composites fabricated at 1923 K, respectively. Based on the colors of scale bar showed on the right of Fig. 6, the concentration of elements distributed in composites can be identified. In Fig. 6(a), the green areas correspond to the carbon-rich areas which comprise carbon fiber and carbon matrix derived from the pyrolysis of phenolic resin. Obviously, the carbon fiber can be identified from its oval shape. For the silicon-rich areas, they can be identified from the Si mapping in Fig. 6(b) and indicated in red colors. Combining Fig. 6(a) with (b), we could know that the SiC matrix distributed in the grey area as shown in Fig. 6(c). In addition, some gaps between the SiC and C matrix were observed. However, while increasing the infiltration temperature to 1973 K, the compositions of constituent phases were changed significantly as shown in Fig. 7.

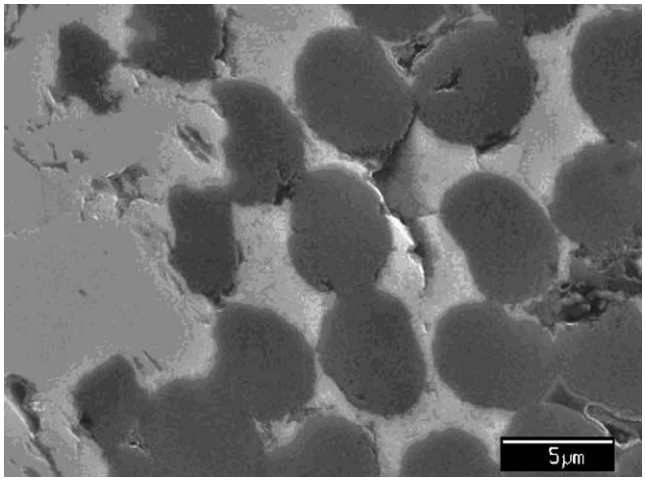

Fig. 3. Morphology of the matrix area for C_f/SiC composite fabricated at 1973 K.

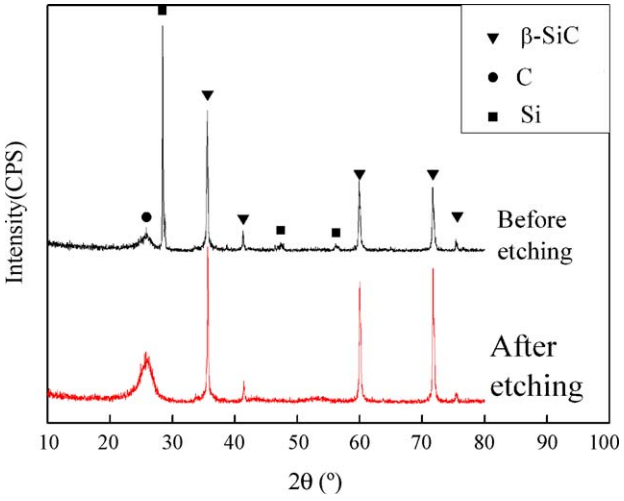

Fig. 4. XRD diffraction patterns of C_f/SiC composites fabricated by VSI process at 1973 K.

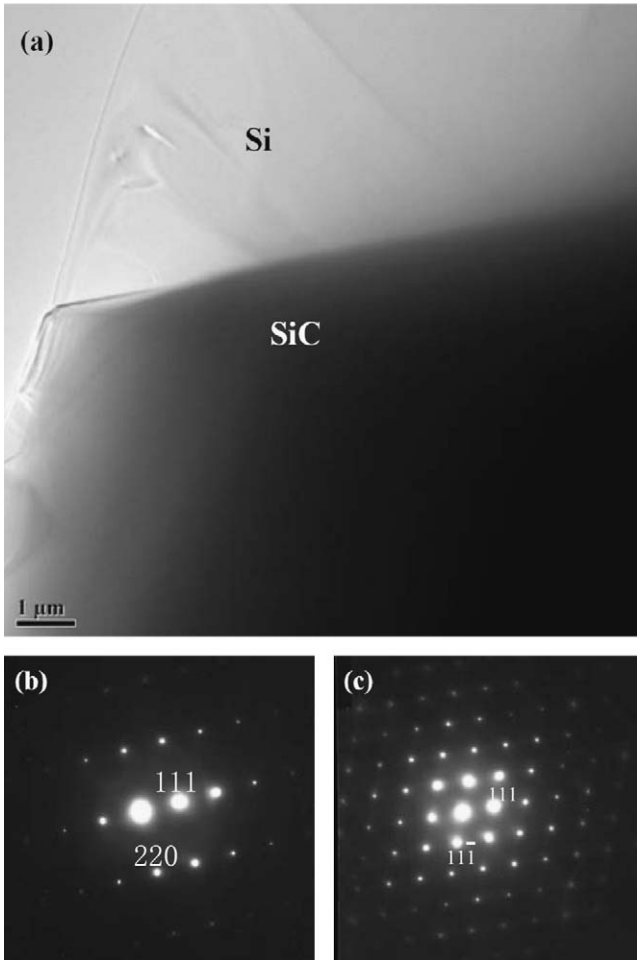

Fig. 5. TEM observation of C_f/SiC composite fabricated at 1973 K: (a) matrix area; (b) SAD pattern for SiC crystal; (c) SAD pattern for Si crystal.

In Fig. 7(a), only intact carbon fibers with oval shape were found, indicating the carbon from the pyrolysis of phenol resin was consumed by the reaction with silicon vapor during VSI process. This result was also evidenced by the Si mapping in Fig. 7(b), but still residual Si was found appearing in red colors. The carbon fiber, SiC matrix and residual Si were presented in black, grey and white colors as shown in Fig. 7(c). Based on the etching result, the volume fraction of residual Si in composite was calculated to be about 14.5%. There are no gaps observed among the different phases.

3.2. Mechanical properties and fracture morphologies

Fig. 8 shows the stress–displacement curve for composites fabricated at 1973 K, which exhibited a non-catastrophic fracture behavior. The ultimate flexural stress is about 238.9 ± 41.2 MPa. Load–displacement curves, obtained from three-point bending tests, were used to obtain work of fracture. The area below the load–displacement curve, when the load dropping down 10% from the peak point, was used to calculate the work of fracture and evaluate the composite toughness. It is about 9.5 kJ/m^2 when the VSI temperature is 1973 K. The morphologies of fracture surfaces were analyzed by SEM observation to understand the fracture behavior.

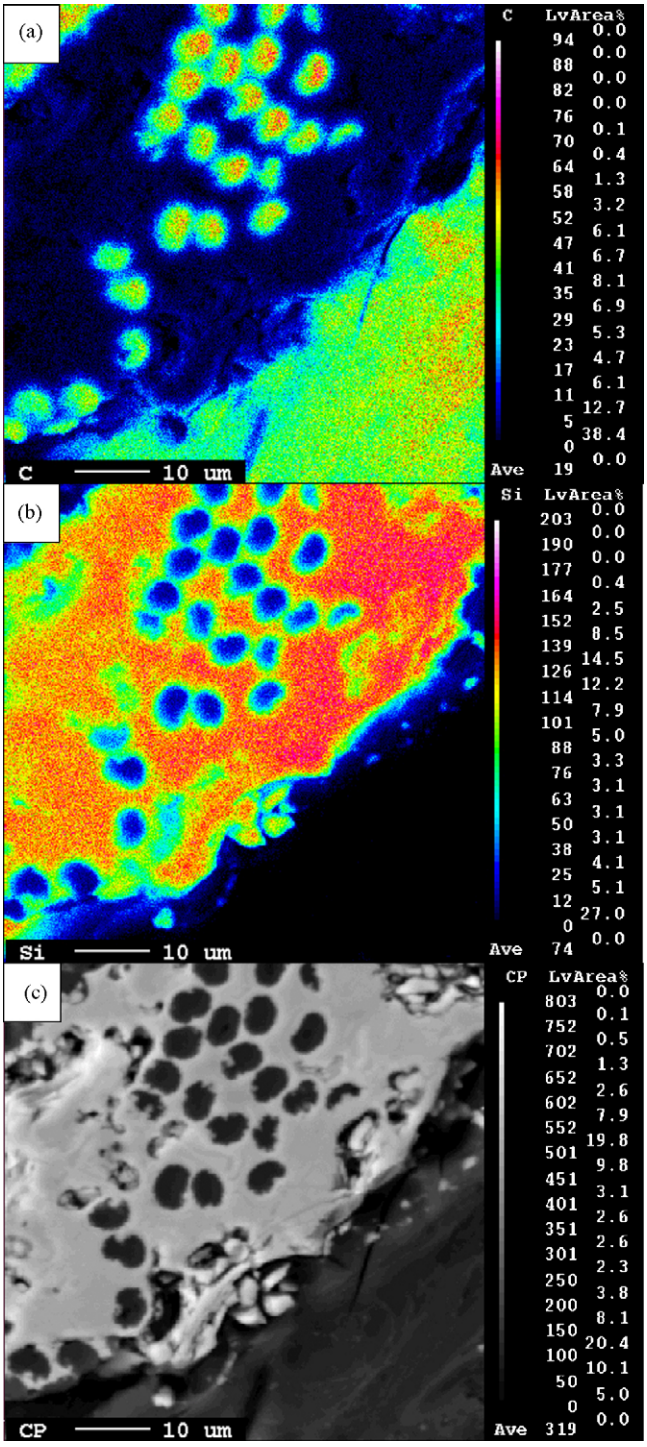

Fig. 6. Element mapping of C_f/SiC composite fabricated at 1923 K: (a) carbon mapping; (b) silicon mapping; (c) distribution of constituent phases.

Fig. 9 shows the morphologies of fracture surface of composites after bending test. It is clear that the PyC and SiC interphase deposited on the carbon fiber are in good condition after VSI process as shown in Fig. 9(a). The thickness is about 150 nm for PyC layer and 250 nm for SiC layer, respectively. In addition, from Fig. 9(b), it can be seen that bi-layered PyC–SiC interphase still remains on the surface of pull-out fibers.

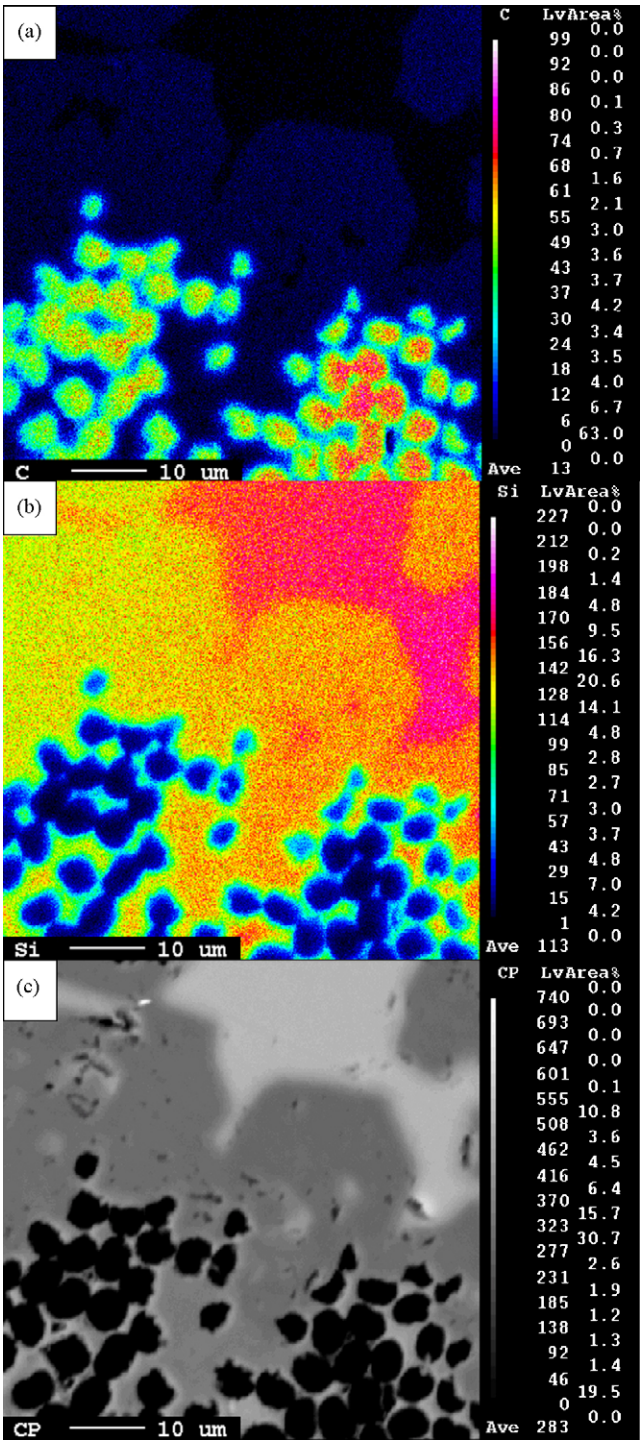

Fig. 7. Element mapping of C_f/SiC composite fabricated at 1973 K: (a) carbon mapping; (b) silicon mapping; (c) distribution of constituent phases.

3.3. Oxidation resistance

Fig. 10 shows the weight change as a function of time for composites fabricated at 1973 K after isothermal exposure at 1273 K in air for 10 h. It is clear that a total weight loss is observed for the composites exposed to such oxidative environment. In C_f/SiC composite, oxidation of PyC layer and carbon fiber led to weight loss, while oxidation of SiC

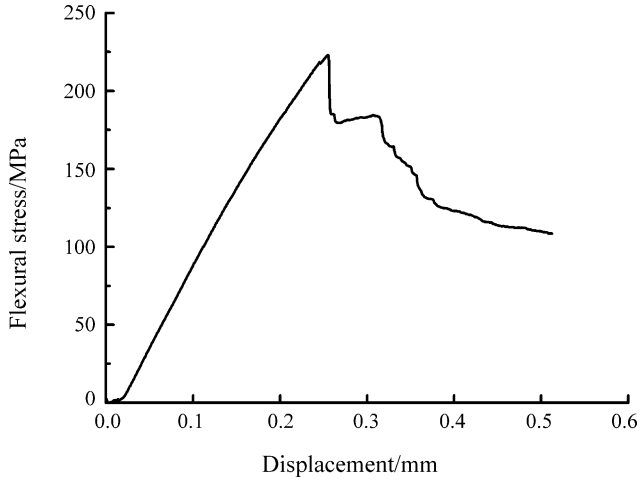

Fig. 8. Stress–displacement curve from three-point bending test for C_f/SiC composite fabricated at 1973 K.

materials (matrix and interphase layer) and residual Si resulted in weight gain. A total weight loss indicated that the weight loss from the oxidation of PyC layer and carbon fibers is higher than weight gain from the oxidation of SiC and Si materials. In other words, the composites are not self-healing. The weight loss is about 3.8% after thermal exposure for 1.5 h, but it is increased to about 13.8% as the exposure time is up to 10 h.

Fig. 11 shows the surface morphologies of composites after thermal exposure at 1273 K in air for 10 h. Many carbon fibers were oxidized and resulted in the formation of cavities along the fiber's longitudinal direction. No obvious changes on the surface of SiC matrix were observed.

4. Discussion

In order to understand the effects of infiltration temperature on the properties of C_f/SiC composite, the basic properties of the C_f/SiC composites fabricated by VSI process at different infiltration temperatures are summarized in Table 1.

It can be seen that there are no obvious differences observed among the preform bodies used for VSI process, but a clear mass gain of preform body is observed after VSI process, being increased from 10% to 18.6% as the temperature increased from 1873 K to 1923 K. Especially, a large mass gain (57.8%) is obtained after VSI process at 1973 K (Fig. 12). Correspondingly, the bulk density of the composites was increased from 1.68 g/cm^3 to 2.25 g/cm^3 as the infiltration temperature increased from 1873 K to 1973 K. And also the open porosity decreased significantly with increasing the infiltration temperature. At 1973 K, the open porosity is 6%, which is much lower than those of composites fabricated by CVI [11,12] and PIP [13] process. It is noted that VSI can be considered as a suitable method for fabrication of dense composites. In order to investigate the evolution of pore network, the microstructure of the preforms at different steps was studied. As the preform had a special fiber distribution (8:2:1 in x:y:z directions), the large pore are presented in the inter-bundle area, while the pores in the intra-bundle area are little. After the slurry impregnation,

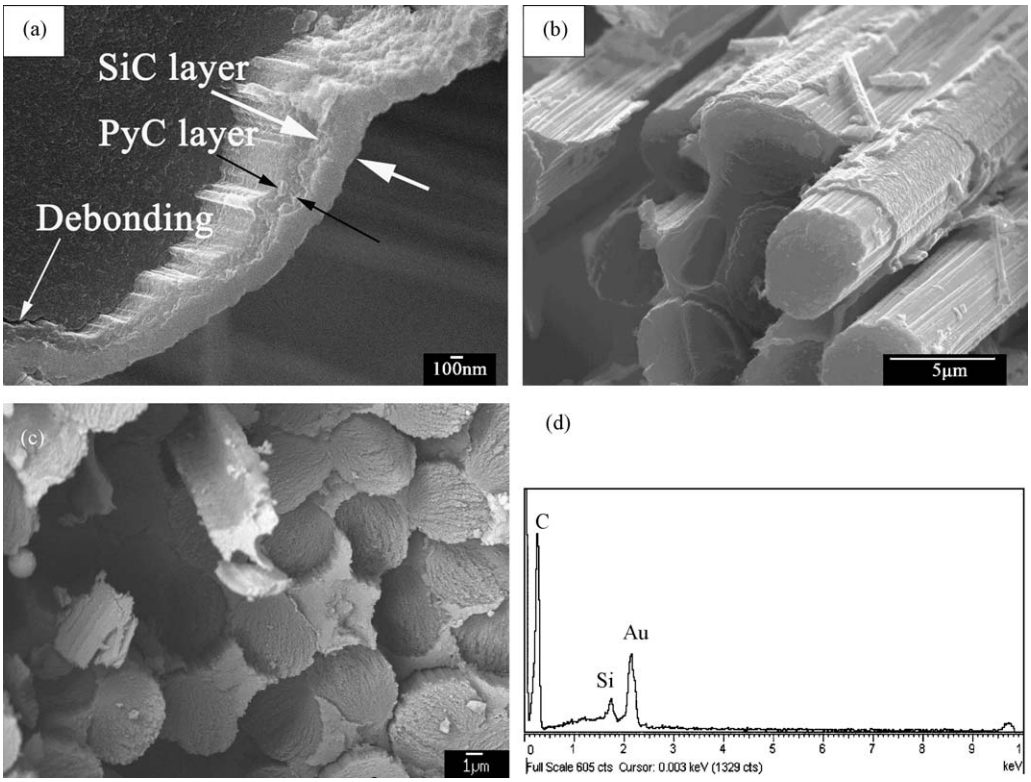

Fig. 9. Bi-layered PyC–SiC interphase and its debonding (a), fiber pull-out (b) of C_f/SiC composites with interphase, siliconized fiber (c) and EDS analysis (d) of C_f/SiC composites without interphase.

different structures are also apparent, as shown in Fig. 13. It is shown that the micropores in the intra-bundle areas mostly are filled with the matrix and there are large pore remaining in the inter-bundle area. However, the lager pores disappeared after VSI, illuminating the large inter-bundle pores can be filled by VSI.

From the SEM observation of crosssection of composites fabricated at different infiltration temperatures as shown in Figs. 2 and 3, it was observed that densification could be improved by increasing the infiltration temperature. This is consistent with the results listed in Table 1. The increased density might be due to the high silicon vapor pressure at high temperature leading to an increased gas phase diffusion of silicon atoms. Spontaneously, the amount of silicon reacted with carbon increased as indicated by the mass gain of preform body in Table 1. The micropores observed in the intra-bundle areas might be caused by the deposition of interphase bi-layer during CVI process. After the deposition of interphase bi-layer, it was found that fibers within a yarn were adhering to each other. As we know, CVI process easily results in the formation of closed micropores [14]. Thus, during the VSI process, the silicon vapor is difficult to infiltrate into the closed micropores in intra-bundle areas.

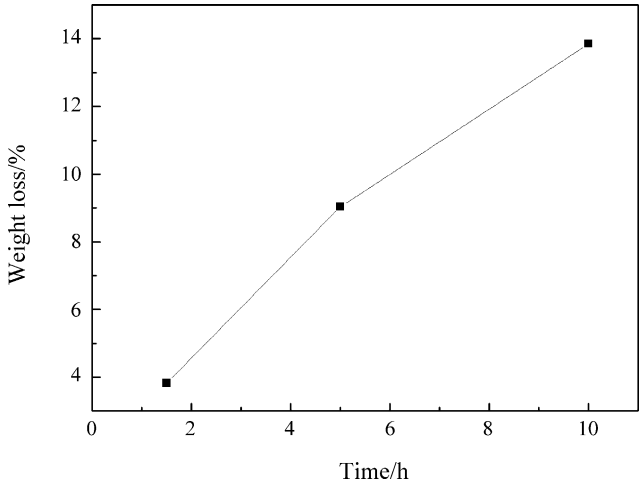

Fig. 10. Weight loss as a function of time for C_f/SiC composite fabricated by VSI at 1973 K after isothermal exposure at 1273 K for 10 h.

The gaps formed between the SiC and C matrix shown in Fig. 6(c), are due to the volume shrinkage during pyrolysis of phenolic resin, but these gaps were filled by silicon after VSI process at high temperatures (see Fig. 7(c)). The infiltrated silicon could improve the gas hermeticity and oxidation resistance.

The infiltration temperature has a strong influence not only on the microstructure, but also on the compositions of constituent phases. From the quantitative results shown in Figs. 6 and 7, it can be seen that the compositions of constituent phases are varied with the temperatures. For the composites fabricated at 1923 K, carbon, silicon and silicon carbide are coexisting in the matrix area. By contrast, when the infiltration temperature is increased to 1973 K, almost no carbon matrix remained, indicating the carbon matrix has completely reacted with the infiltrated silicon to form the SiC matrix. The residual Si in composites is attributed to the silicon vapor condensation

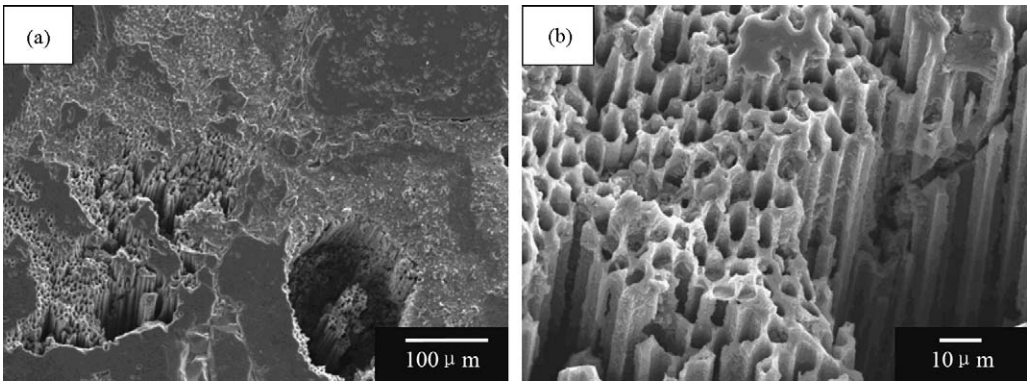

Fig. 11. Morphologies of C_f/SiC composites after isothermal exposure test at 1273 K for 10 h.

Table 1
Properties of C_f/SiC composites fabricated by VSI at different infiltration temperatures.

VSI temperature (K)	1873	1923	1973
Density of preform before VSI (g/cm^3)	1.51	1.56	1.52
Mass gain of the preform (%)	10.7	18.6	57.8
Density of VSI composites (g/cm^3)	1.68	1.87	2.25
Open porosity (%)	27.76	19.50	5.99
Residual Si content (vol.%)	–	–	14.5
Flexure strength (MPa)	149.0 ± 13.3	239.5 ± 35.6	238.9 ± 41.2
Work of fracture (kJ/m^2)	–	–	9.5

during the cooling of VSI process. As mentioned before, the filling of Si in pores/cracks would be beneficial to the improvement of gas hermeticity and oxidation resistance.

By means of XRD and TEM analysis (Figs. 4 and 5), only β-SiC crystals were formed during the VSI process. There are no α-SiC peaks detected. Indicating no phase transition of SiC occurred during the process even for infiltration temperature as high as 1973 K. However, the phase transition from β-SiC to α-SiC probably happens in LSI process due to the violent temperature increase caused by significant exothermic effect [15,16]. From the viewpoint of microstructure, 1973 K is a suitable temperature to form the SiC matrix.

Furthermore, the results of bending tests listed in Table 1, shows that the ultimate flexural stress is the least when the VSI temperature is the lowest (1873 K), accompanying with the least density, but the ultimate flexural stresses are very similar when VSI temperature are 1923 K and 1973 K. This might be due to the large amount of residual silicon and its inhomogeneous distribution in composite. As we know, when the silicon is transformed from liquid to solid state during cooling process, a volume expansion of about 8% occurs. Such volume expansion will apply a tension residual stress to SiC matrix, resulting in a decreased flexural stress. The later experiments also showed high strength (∼500 MPa) after the silicon content was decreased, but the detailed study would be carried on. The non-catastrophic fracture behavior indicated that crack deflection along the interphase between carbon fiber

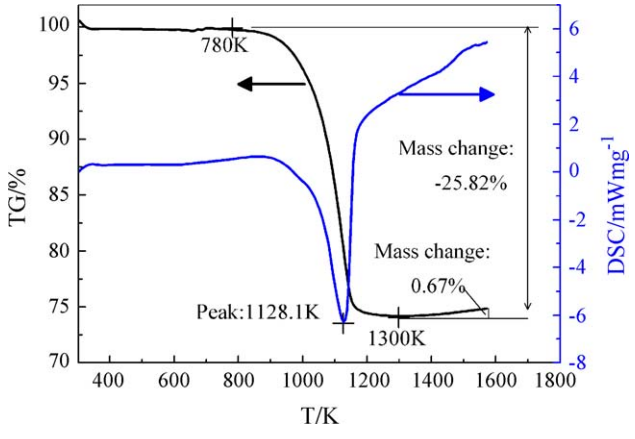

Fig. 12. TG–DSC curve obtained at elevated temperatures for C_f/SiC composite fabricated at 1973 K.

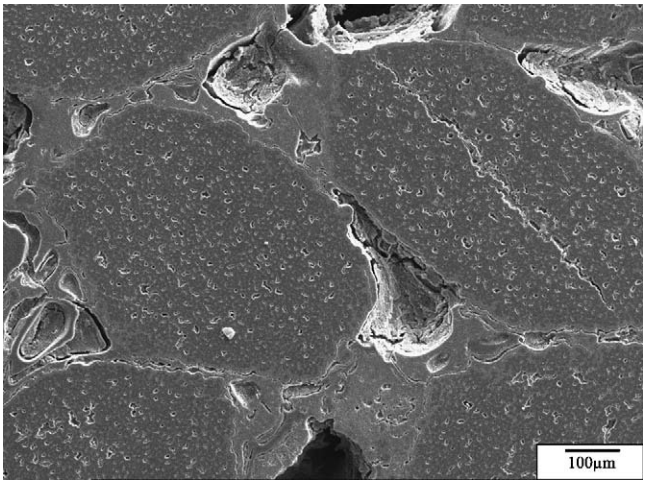

Fig. 13. Microstructure of C_f/SiC composites before VSI.

and matrix must have occurred, as shown by the interphase debonding and fiber pull-out in Fig. 9. It was thought in the present work the bi-layered PyC–SiC interphase could protect the carbon fibers from the reaction with silicon during VSI process. The silicon vapor reacts not only with the carbon matrix, but also with carbon fibers. The reaction between carbon fiber and silicon could decrease the fiber strength and increase the bonding strength between fiber and matrix. Siliconized carbon fiber and flat fracture surface were observed in the previous work when the fiber was not protected, as shown in Fig. 9(c). Fiber surface becomes rough and there are little fiber pull-outs. The energy diffraction spectra (EDS) analysis (Fig. 9(d)) shows there is silicon element in the fiber. It is illuminated that gaseous silicon reacts with carbon fiber unless there are protecting interphases. The intact carbon fibers observed in Fig. 9(b) evidence that the bi-layered PyC–SiC interphase could isolate the carbon fiber from silicon vapor and improve the fracture toughness. The modest flexural stress (Fig. 8) and fiber pull-out in Fig. 9(b) further convinced that the PyC–SiC interphase plays an active role in the fracture behavior of C_f/SiC composites by VSI process.

When the composite was exposed to oxidative environments, the formation of silica from the oxidation of SiC and residual Si could theoretically stop the oxygen attack of carbon materials including the carbon fiber and PyC interphase, resulting in an improved oxidation resistance. As observed in Figs. 10 and 11, the matrix area does not show obvious morphologies change, but the burning of carbon fiber formed many hollow holes and resulted in a weight loss. It was expected that the weight loss will decrease at high temperatures because of the quick formation of silica. The quick formation of silica reduced the exposure areas of composite to oxidative environment. On the other hand, the TG–DSC data for the C_f/SiC composites fabricated at 1973 K was used to better understand the oxidation behavior (see Fig. 12). From the TG curve, it can be seen that the weight loss started at 780 K due to the oxidation of carbon fiber. The weight loss reached a maximum (25.82%) at 1300 K. However, at temperatures above 1300 K, the weight loss slightly decreased, indicating the weight gain from the formation of SiO_2 is somewhat higher than the weight loss from the oxidation of carbon fiber. If the mass at 1300 K is chosen as the reference value, a mass gain of about 0.67% is obtained at 1573 K. Such mass gain is due to the quick formation of silica which decreases the oxidation rate of carbon fibers.

The weight loss from TG–DSC test was much higher than that from isothermal exposure test. This is due to the volume fraction of carbon fiber exposed to air in the specimen used for TG–DSC test is larger than that of specimen used for isothermal exposure tests. Even so, from TG curve, the variation tendency of mass change in the present test condition was observed and used for the further optimization of process.

5. Conclusions

Three-dimensional (3D) carbon fiber-reinforced SiC matrix composites were fabricated by vapor silicon infiltration process at different infiltration temperatures. The main results are summarized as follows:

(1) The analysis of microstructure and constituent phases by means of SEM, TEM and WDS, revealed that SiC matrix could be formed by VSI process effectively. Especially, the inter-bundle area is prone to be densified.
(2) The distribution and composition of constituent phases are dependent on the silicon vapor infiltration temperatures. At 1923 K, there are large mount of residual carbon and gaps in the matrix. However, there are little residual carbon matrix when the VSI temperature is 1973 K. The matrix consists of SiC and residual Si. The properties of composite could be improved by further design and optimization of process route.
(3) The densities of fabricated composites increase with increasing the infiltration temperature, which is about 2.25 g/cm^3 for composite fabricated at 1973 K.
(4) The stress–displacement curve of composites showed a non-catastrophic fracture behavior. For composite fabricated at 1973 K, the ultimate flexural stress is about 238.9 ± 41.2 MPa, which is comparable to those of composites fabricated by other processing techniques, demonstrating the VSI process is an effective way to fabricate dense C_f/SiC composites with good mechanical properties.

Acknowledgements

This work was supported by the National Natural Science Foundation Program of China under Grant No. 50472015 and the National High Technology Research and Development Program of China (863 Program) under Project No. 2006AA03Z565.

The authors wish to thank Dr. Jianjun Sha for his invaluable contributions to the present work.

References

[1] A. Mühlratzer, H. Pfeiffer, CMC body flaps for the X-38 experimental space vehicle, Ceram. Eng. Sci. Proc. 23 (3) (2002) 331–338.
[2] F. Christin, A global approach to fiber nD architectures and self-sealing matrices: from research to production, Int. J. Appl. Ceram. Technol. 2 (2) (2005) 97–104.
[3] R. Naslain, SiC-matrix composites: nonbrittle ceramics for thermo-structural application, Int. J. Appl. Ceram. Technol. 2 (2) (2005) 75–84.
[4] R. Naslain, Design, preparation and properties of non-oxide CMCs for application in engines and nuclear reactors: an overview, Compos. Sci. Technol. 64 (2) (2004) 155–170.
[5] W. Krenkel, Carbon fiber reinforced CMC for high-performance structures, Int. J. Appl. Ceram. Tchnol. 1 (2) (2004) 188–200.
[6] S.P. Lee, Y. Katoh, A. Kohyama, Development of SiC_f/SiC composites by the melt infiltration process, Ceram. Trans. 144 (2002) 115–122.
[7] Y. Chiang, R. Messner, C. Terwilliger, Reaction-formed silicon carbide, Mater. Sci. Eng. A 144 (1–2) (1991) 63–74.
[8] Y. Wang, S. Tan, D. Jiang, Effect of porous carbon preform and the infiltration process on the properties of reaction-formed SiC, Carbon 42 (2004) 1833–1839.
[9] Q. Zhou, S. Dong, X. Zhang, Y. Ding, Z. Huang, D. Jiang, Synthesis of the fiber coating by FP-CVI process, Key Eng. Mater. 336–338 (2007) 1307–1309.

[10] http://webbook.nist.gov/cgi/cbook.cgi?ID=C7440213&Units=SI&Mask=7&Type=ANTOINE&Plot=on#ref-1.
[11] L. Yan, W. Zou, M. Song, T. Wang, L. Fu, Effect of reaction gas mixing ratio on deposition performance of C/SiC in ICVI Process, J. Solid Rocket Technol. 25 (3) (2002) 59–62.
[12] S. Tang, J. Deng, H. Du, W. Liu, K. Yang, Fabrication and microstructure of C/SiC composites using a novel heaterless chemical vapor infiltration technique, J. Am. Ceram. Soc. 88 (11) (2005) 3253–3255.
[13] G. Zheng, H. Sano, Y. Uchiyama, K. Kobayashi, K. Suzuki, H. Cheng, Preparation and fracture behavior of carbon fiber/SiC composites by multiple impregnation and pyrolysis of polycarbosilane, J. Ceram. Soc. Jpn. 106 (12) (1998) 1155–1161.
[14] R. Naslain, F. Langlais, R. Pailler, G. Vignoles, Processing of SiC/SiC fibrous composites according to CVI-techniques, Ceram. Trans. 144 (2002) 19–37.
[15] S. Shinozeki, J. Noakes, Recrystallization and phase transformation in reaction-sintered SiC, J. Am. Ceram. Soc. 61 (5–6) (1978) 237–242.
[16] J. Schulte-Fischedick, A. Zern, J. Mayer, M. Rühle, M. Frieß, W. Krenkel, R. Kochendörfer, The morphology of silicon carbide in C/C–SiC composites, Mater. Sci. Eng. A 332 (2002) 146–152.